Alignment of Copolymer Morphology by Planar Step Elongation during Spinodal Self-Assembly

Marcus Müller[1,*] and Jiuzhou Tang[2]
[1]Institute for Theoretical Physics, Georg-August University, 37077 Göttingen, Germany
[2]State Key Laboratory of Polymer Physics and Chemistry, Institute of Chemistry, Chinese Academy of Sciences, Beijing 100190, China
(Received 9 September 2015; revised manuscript received 20 October 2015; published 23 November 2015)

Using simulation and numerical self-consistent field theory of an unentangled diblock copolymer melt, we study the interplay between relaxation of molecular conformations from a highly stretched, nonequilibrium state and structure formation of the local, conserved density during self-assembly from a disordered state. We observe that the planar elongation of molecular conformations in the initial, disordered state results in an alignment of lamella normals perpendicular to the stretch direction during the subsequent self-assembly. Although thermodynamically the parallel orientation is favored, the alignment of the lamella normal perpendicular to the stretch direction is characterized by the larger growth rate of composition fluctuations during the spinodal ordering process.

DOI: 10.1103/PhysRevLett.115.228301 PACS numbers: 82.35.Lr, 64.60.Cn, 82.35.Jk, 83.50.Uv

Copolymer materials have attracted abiding interest for their ability to self-assemble into spatially modulated structures with a characteristic periodicity of nanometers. The spontaneous structure formation, however, often results in fingerprint-like patterns that are riddled with defects and feature grains of different orientations [1]. Abiding effort has been devoted to direct the self-assembly into aligned thin-film structures by external fields like chemical [2–4] or topographical surface patterns [5,6], electric [7–9] or magnetic [10,11] fields, or shear flow [12–16]. All these directing fields are *quasistatic*, i.e., in the presence of the directing field the copolymer system reaches a time-independent, stationary morphology that, ideally, is independent from the initial state.

We explore how a stepwise mechanical deformation in the initial, disordered state directs the self-assembly of copolymers. Such a step deformation can be produced by roll casting [17–19], where a solvent-swollen polymer film is mechanically elongated and, subsequently, self-assembles as the solvent evaporates. A similar molecular deformation occurs during melt drawing [20]. In both cases, experiments observe the alignment of lamella planes or cylinders along the stretch direction. The alignment mechanism, however, is only incompletely understood. Alternatively, one could mechanically deform a disordered copolymer film in a glassy or tightly cross-linked state and investigate the self-assembly after heating above the glass transition temperature or releasing the cross-links, respectively. A related mechanical deformation also occurs in nanoimprint lithography, where a copolymer film is embossed by a topographically pattern mold [21] and, in addition to the shape of the mold, the molecular deformation may affect the morphology.

In general, the theoretical description of the interplay between relaxation of chain conformations from a nonequilibrium, stretched state and structure formation of the local composition, $\phi_A(\mathbf{r})$, during self-assembly is a challenge. A step deformation may serve as a test bed for theoretical approaches because, as demonstrated below (i) the relaxation of molecular conformations is largely unaffected by incipient composition fluctuations, and (ii), the spatially uniform deformation does not give rise to stress gradients and concomitant flows.

In dynamical self-consistent field theory, the conserved density is routinely considered as the *only* slow variable, i.e., the chain conformations are assumed to be in equilibrium with the instantaneous $\phi_A(\mathbf{r})$. During spinodal structure formation, however, this assumption fails [22]: The relaxation of the large-scale molecular conformations is dictated by the Rouse time, $\tau_R = {R_{eo}}^2/3\pi^2 D$, where R_{eo} denotes the unperturbed end-to-end distance and D the single-chain self-diffusion coefficient, respectively. The same time scale characterizes the initial, spinodal stage of self-assembly, during which the composition inside domains approaches its saturation value and interfaces form. Here, we explore how to account for time-dependent molecular conformations, which are not in equilibrium with the instantaneous composition.

We use particle-based simulation and self-consistent field theory (SCFT) of a soft, coarse-grained model [23–25] to study the kinetics and thermodynamics, respectively. The symmetric AB diblock copolymers are discretized into $N = 32 + 32$ segments. The bonded interactions are given by the discretized Edwards Hamiltonian, $\mathcal{H}_b = (3k_BT/2{b_o}^2)\sum_{i=1}^{n}\sum_{s=1}^{N-1}\mathbf{b}_i^2(s)$ with $b_o = R_{eo}/\sqrt{N-1}$. $\mathbf{r}_i(s)$ denotes the position of the sth segment on chain i, and $\mathbf{b}_i(s) = \mathbf{r}_i(s+1) - \mathbf{r}_i(s)$. Nonbonded interactions are expressed via a density functional $\mathcal{H}_{\rm nb}/k_BT\sqrt{\bar{N}} = \int(d\mathbf{r}^3/{R_{eo}}^3)[(\kappa N/2)(\hat{\phi}_A + \hat{\phi}_B - 1)^2 - (\chi N/4)(\hat{\phi}_A - \hat{\phi}_B)^2]$

with invariant degree of polymerization, $\bar{\mathcal{N}} = (\rho R_{eo}{}^3/N)^2 = 128^2$, and ρ being the segment number density. The local A density is calculated from the molecular conformations, $\hat{\phi}_A(\mathbf{r}|\{\mathbf{r}\}) = (1/\rho)\sum_{i=1}^{n}\sum_{s=1}^{N/2}\delta(\mathbf{r}-\mathbf{r}_i(s))$ and similarly for the B density. The inverse isothermal compressibility $\kappa N = 50$ limits density fluctuations, and χN quantifies the thermodynamic incompatibility of the blocks [26].

The kinetics of self-assembly is investigated by single-chain-in-mean-field simulation [23,25]. We use Smart Monte Carlo moves [46] that employ the strong bonded forces to propose a local trial displacement. The dynamics of this force-bias algorithm is virtually identical to Brownian dynamics beyond 100 Monte Carlo steps [47]. Since the soft, nonbonded interactions do not enforce noncrossability, there are no entanglements, and the single-chain dynamics in the disordered melt agrees with the Rouse model [47]. From the self-diffusion coefficient D at $\chi N = 0$ we extract the Rouse time, $\tau_R = 1204$ Monte Carlo steps. τ_R sets the unit of time.

Particle-based simulation.—We consider the following self-assembly process: First, a thin film with thickness $D = 10R_{eo}$ and lateral extensions $L_y = L_z = 7.9R_{eo}$ is equilibrated [48]. The confining film surfaces are impenetrable and nonpreferential, while periodic boundary conditions are applied in the lateral directions, y and z. Second, by rescaling the explicit particle coordinates, we compress the film thickness D instantaneously by a factor $1/\lambda = 0.1$ and elongate the spatial extension in the y direction L_y by λ, leaving the perpendicular system size L_z and volume V unaltered. This affine planar deformation mimics the stretching during roll casting and is qualitatively similar to the uniaxial deformation during melt drawing. Third, we instantaneously quench the system from the disordered into the microphase-separated state $\chi N = 0 \rightarrow 20$, representing the start $t = 0$ of self-assembly after solvent evaporation. Subsequently, we investigate the kinetics of structure formation from this nonequilibrium starting point where both (i) the molecular conformations are deformed and (ii) the disordered morphology is unstable.

Figure 1 presents the time evolution of composition in the lateral yz plane. In the first snapshots, $t/\tau_R \leq 2$, composition fluctuations spontaneously grow and the composition saturates inside the domains. This behavior characterizes the spinodal regime. The stretched starting configuration imparts an anisotropy onto composition fluctuations, giving rise to a preferential alignment of the nascent AB interfaces along the stretch direction y. Figure 1 also shows the collective structure factor $S_{\mathrm{coll}}(\mathbf{q})$ of composition fluctuations with wave vectors perpendicular to and along the stretch direction. Composition fluctuations with $\mathbf{q}$ along the z direction grow significantly more rapidly than those along the stretch direction, y. Subsequently, these internal AB interfaces sharpen and the order improves by defect annihilation. The overall morphology exhibits a preferred

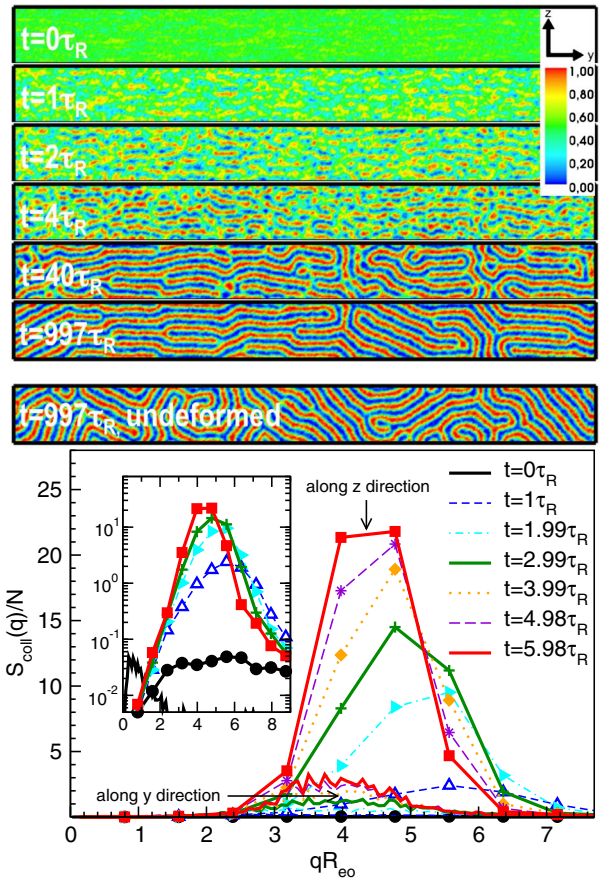

FIG. 1 (color online). Top: Time evolution of composition fluctuations in a slice perpendicular to the x direction as obtained by MC simulation. The bottom image presents, for comparison, the fingerprint pattern (at $t/\tau_R = 997$) obtained by quenching the system from $\chi N = 0$ to 20 without initial deformation. Bottom: Time dependence of the collective structure factor along the stretch direction (lines) and perpendicular (symbols) to it, averaged over 32 independent simulation runs. The inset presents $S_{\mathrm{coll}}(q_z)/N$ on a logarithmic scale to indicate the exponential growth for $t \leq 2\tau_R$.

orientation of lamellar normals along the z direction, in accord with roll-casting and melt-drawing experiments [17–20]; however, it lacks perfect long-range order because stretching does not facilitate spatial registration of domains.

Anisotropic Gaussian chains at $t = 0$.—Several strategies have been devised to account for the molecular strain or the thermodynamically conjugated stress. Fredrickson [49] and Kawakatsu and co-workers [50] included the virial stress, $\sigma_{\alpha\beta}$ (where Greek indices refer to Cartesian components), as additional collective variable in the SCFT free-energy functional $\mathcal{F}[\phi_A, \sigma_{\alpha\beta}]$. For Gaussian chains with zero-ranged interactions, $\sigma_{\alpha\beta} = (3k_BT/Vb_o{}^2)\sum_{i,s} b_{i\alpha}(s)b_{i\beta}(s)$ is related to the anisotropic distribution of bond lengths and directions. Since it only involves local information along the molecular contour, a Markovian description of conformations is retained. In the initial, disordered melt, $t = 0$, the spatially

uniform but anisotropic stress (or strain) decreases the conformational entropy but does not qualitatively alter the Gaussian chain statistics; i.e., the single-chain conformations obey an anisotropic Gaussian distribution, $\mathcal{P}_o \sim \exp\{-\sum_{s,\alpha}[3b_{i\alpha}^2(s)/2{b_{o\alpha}}^2]\}$, with $b_{ox} = b_o/\lambda$, $b_{oy} = b_o\lambda$, and $b_{oz} = b_o$ for all chains i.

The negative inverse, $-1/S_{\mathrm{coll}}(\mathbf{q})$, of the collective structure factor quantifies the thermodynamic driving force for the spontaneous growth of composition fluctuations with wave vector $\mathbf{q}$. For anisotropic Gaussian chains, $S_{\mathrm{coll}}(q_\alpha) = N\tilde{S}(\chi N, q_\alpha b_{o\alpha}\sqrt{N-1})$. The scaling function $\tilde{S}$ does not depend on the Cartesian direction α; i.e., the structure factor along and perpendicular to the stretch direction will be identical if we rescale the length scale by the corresponding statistical segment length (cf. inset of Fig. 1, bottom). Likewise, if we use anisotropic Gaussian chains $\mathcal{P}_o$ within SCFT [51], the excess free energy, Δf, per macromolecule in the lamellar phase with normal α and periodicity L_α, will obey $\Delta f = k_B T \tilde{f}(\chi N, b_{o\alpha}\sqrt{N-1}/L_\alpha)$; i.e., for $L_y = \lambda L_z$, lamellar phases with normals in y and z directions have identical free energy. Thus, the anisotropic Gaussian conformations at $t = 0$ do not result in a thermodynamic preference for a particular direction $\alpha = y$ or z.

Non-Gaussian chains.—At later times, the chain conformations relax. Since $b_{i\beta}(s)b_{i\gamma}(s)$ contains all Rouse modes, $\mathbf{X}_p = (1/N)\sum_{s=1}^{N}[\mathbf{r}(s)/R_{eo}]\cos[(\pi p/N)(s-\frac{1}{2})]$, and Rouse modes with different indices p have different relaxation times $\tau_p = \tau_{\mathrm{R}}/p^2$ [52,53]—the conformational statistics for $t > 0$ deviates from an anisotropic Gaussian chain: On large length scales, the conformations will longer retain the initial, elongated shape, whereas the small-scale structure will rapidly relax towards the isotropic Gaussian distribution with equilibrium statistical segment length b_o. We quantify this non-Gaussianity of molecular conformations by the ratio of variances of the first two Rouse modes $\langle X_{1y}^2\rangle/4\langle X_{2y}^2\rangle$, which adopts the value 1 for Gaussian chains. The right inset of Fig. 2 demonstrates that this quantity strongly deviates from unity in the spinodal regime $t \approx \tau_R$.

In Fig. 2 we analyze the time evolution of the first 4 Rouse modes. The variances of individual modes decay exponentially in time. Retaining the slowest, first Rouse mode and assuming higher order modes to be equilibrated provides an appropriate approximation on the time scale of spinodal self-assembly, $t \approx \tau_R$. Quantitatively, the relaxation times τ_p are very close to the predictions of the Rouse model for the disordered melt because (i) composition fluctuations have not yet fully developed by the time X_{1y}^2 has decayed and (ii) the bonded forces that define the molecular architecture are stronger than the nonbonded forces. Even if we start with an equilibrated melt at $\chi N = 9$ (instead of $\chi N = 0$ in order to account for the frozen-in fluctuations of the as-cast film), the stronger composition

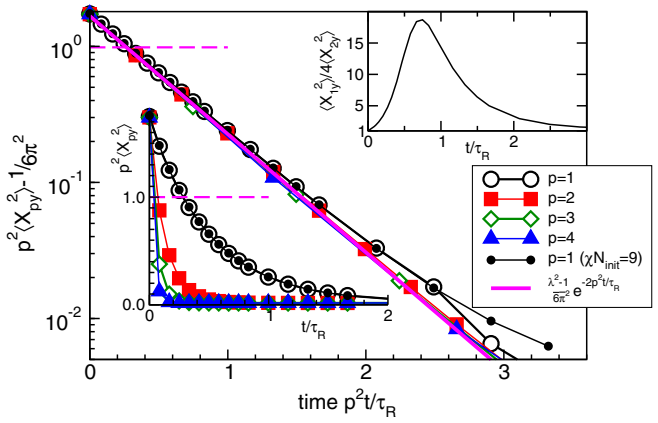

FIG. 2 (color online). Relaxation of variance of Rouse modes X_{py}^2 along the stretch direction during structure formation. Similar to the disordered system, the individual modes relax exponentially with characteristic time $\tau_p = \tau_R/p^2$. The right inset quantifies the time-dependent non-Gaussianity of the molecular conformations.

fluctuations at $t = 0$ will not significantly affect the single-chain dynamics.

Ilg, Öttinger, and Kröger employed the tensor of gyration to describe the large-scale deformation of macromolecular conformations in shear flow [54] and, in the same spirit, we propose to retain both the conserved density ϕ_A *and* the variance of the slowest Rouse modes $X_{1\alpha}X_{1\beta}$, as slow collective variables of the free-energy functional $\mathcal{F}[\phi_A, X_{1\alpha}X_{1\beta}]$.

Thermodynamics.—To investigate the thermodynamic consequences of non-Gaussian conformations, we describe the base statistics $\mathcal{P}_o[\{\mathbf{r}\}]$ of noninteracting single-chain conformations by specifying the variance of Rouse modes. We set $\langle X_{1y}^2\rangle_0 = 1$, which is a representative value during the early spinodal regime (cf. Fig. 2), whereas all other variances adopt their equilibrium values [55] $\langle X_{p\alpha}X_{q\beta}\rangle = [(\delta_{pq}\delta_{\alpha\beta})/(6\pi^2p^2)][N/(N-1)][(\pi p)/(2N\sin(\pi p/2N))]^2$.

Constraining Rouse modes, we destroy the Markov character of chain conformations. Thus a partial enumeration scheme [56–58] for an incompressible diblock copolymer melt is employed to compute the collective structure factor and the excess free energy Δf of the lamellar phase at $\chi N = 20$ within SCFT (see the Supplemental Material [26]). To this end, we generate $n = 99\,840\,000$ independent single-chain conformations according to $\mathbf{r}(s)/R_{eo} = \mathbf{X}_0 + 2\sum_{p=1}^{N-1}\mathbf{X}_p\cos[(\pi p/N)(s-\frac{1}{2})]$.

Figure 3 presents Δf for molecules with constraint $\langle X_{1y}^2\rangle_o$ along the lamella normal. Since the Cartesian directions decouple, results for Gaussian chains, $\langle X_{1y}^2\rangle_o = 0.017$, apply to the lamellar phase with normal z in our simulation, whereas $\langle X_{1y}^2\rangle_o = 1$ corresponds to alignment of the normal along the y direction. The lamella periodicity L increases with $\langle X_{1y}^2\rangle_o$, but the behavior differs from that of (anisotropic) Gaussian chains: (i) The preferred

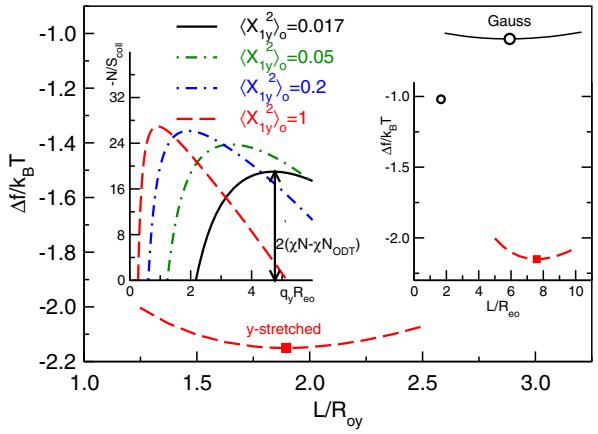

FIG. 3 (color online). Free energy Δf vs lamellar spacing L for molecular conformations with constraint variance of the first Rouse mode along the lamella normal y: Gaussian chains $\langle X^2_{1y}\rangle_o = 0.01715$ and non-Gaussian conformations $\langle X^2_{1y}\rangle_o = 1$ at $\chi N = 20$. The equilibrium spacings are $L_0/R_{eo} \approx 1.67$ and 7.60, and the (base) chain extensions along the lamella normal are $R_{oy}/R_{eo} = 1/\sqrt{3}$ and 4.0, respectively. The left inset depicts the negative, inverse structure factor $-N/S_{\rm coll}$ for various values of $\langle X^2_{1y}\rangle_o$ as indicated in the key.

L is not merely proportional to the chain extension R_{oy} (of noninteracting molecules characterized by $\mathcal{P}_o$), but L_y/R_{oy} decreases upon increasing $\langle X^2_{1y}\rangle_o$ and (ii) the excess free energy Δf decreases in turn. This finding is expected because the macromolecules in the lamellae are stretched along the lamella normal. For Gaussian chains, we find that $\langle X^2_{1y}\rangle_{\rm lam} = 0.0384$ is about twice as large at $\chi N = 20$ as the variance of the base distribution $\langle X^2_{1y}\rangle_o \approx 1/6\pi^2$, and for the highly stretched conformations we observe $\langle X^2_{1y}\rangle_{\rm lam} = 1.1139 > \langle X^2_{1y}\rangle_o = 1$.

Using a large set of single-chain conformations, we also computed $[N/S^{\rm RPA}_{\rm coll}(\mathbf{q})] = \{(S_{AA}+2S_{AB}+S_{BB})/[(S_{AA}S_{BB}-S^2_{AB})/N]\} - 2\chi N$ in the initial, disordered state at $\chi N = 20$ according to the random-phase approximation [59]. The inset of Fig. 3 demonstrates that the thermodynamic driving force $-1/S_{\rm coll}$ of composition fluctuations is larger for modes with $\mathbf{q}$ along the stretch direction y than those along the unaltered direction z. The disordered state becomes unstable at an incompatibility $\chi N_{\rm ODT}$, where the maximum of $-1/S_{\rm coll}$ with respect to q vanishes. The data show that microphase separation already starts at $\chi N_{\rm ODT} \approx 6.5$ for non-Gaussian chains with $\langle X^2_{1y}\rangle_o = 1$ (compared to $\chi N_{\rm ODT} \approx 10.5$ for Gaussian chains).

Thus, the thermodynamic driving force of spontaneously growing fluctuations in the disordered state as well as the free energy of (hypothetical) equilibrium lamellae built by deformed chain conformations with $\langle X^2_{1y}\rangle_o = 1$ favor an alignment of the lamella normal along the stretch direction —opposite to what is observed in experiments [17–20] and our simulation (cf. Fig. 1). Therefore, the observed orientation cannot be explained by thermodynamic considerations $\mathcal{F}[\phi_A, X^2_{1y}]$ alone.

Kinetics.—A complete theory [49,50] also describes the dynamics of the slow, collective variables $\phi_A(\mathbf{r})$ and X^2_{1y}. For our problem, Fig. 2 demonstrates that the single-chain dynamics remains unaffected by the growth of composition fluctuations in the spinodal regime and obeys Rouse behavior. In turn, we also do not expect that a *spatially homogeneous*, single-chain deformation and relaxation induces a composition current. Thus, the spinodal dynamics of composition fluctuations can be described by model B according to the classification of Hohenberg and Halperin [60]

$$\frac{\partial \phi_A(\mathbf{q},t)}{\partial t} = -\Lambda \mathbf{q}^2 {R_{eo}}^2 \frac{N}{S^{\rm RPA}_{\rm coll}(\mathbf{q})} \phi_A(\mathbf{q},t), \qquad (1)$$

where the q^2 factor arises from the diffusive dynamics, and we neglect the wave vector dependence of the Onsager coefficient $\Lambda \sim 1/\tau_R$ [61]. Thermodynamics favors the formation of lamellae with normals along the stretch direction y, but the concomitant lamellar spacing is larger than the preferred spacing along the perpendicular direction z. Thus, as sketched in Fig. 4 (left), the formation of the lamellar structure involves larger-scale rearrangements for lamellae with y normals than for lamellae with perpendicular orientation. We quantify this rational in panel (b), plotting the right-hand side of Eq. (1). Indeed, we observe that the growth rate of composition fluctuations with $\mathbf{q}$ along the z direction is largest in accord with experiments and simulation. Thus, the diffusive dynamics favors the ordering with the shorter lamellar period over the thermodynamically preferred orientation with the longer periodicity along the stretch direction.

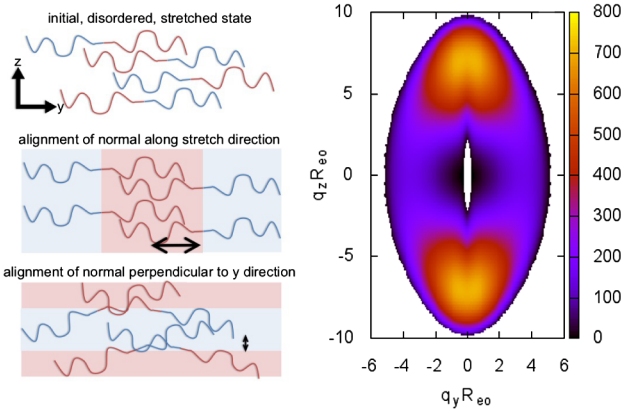

FIG. 4 (color online). Left: Illustration of parallel and perpendicular ordering. The arrows indicate the typical displacement necessary to form the lamellar structure. Right: Contour plot of the growth rate $R(\mathbf{q}) \sim -\{\mathbf{q}^2 {R_{eo}}^2/[S_{\rm coll}(\mathbf{q})/N]\}$ of composition fluctuations in the stretch direction q_y and the perpendicular direction q_z at $\chi N = 20$ and $\langle X^2_{1y}\rangle_o = 1$. Only wave vectors, for which composition fluctuations spontaneously grow, are shown.

In summary, we studied the interplay between relaxation of molecular conformations after an initial stepwise elongation and kinetics of composition fluctuations. Molecular conformations temporarily deviate from an anisotropic Gaussian behavior, and (i) we present evidence that the variance of the first Rouse modes provides an appropriate slow variable in addition to the conserved density. Whereas, the nonequilibrium molecular conformations favor alignment of the lamellar normals along the stretch directions, (ii) the orientation observed in the simulation is dictated by the diffusive kinetics. We expect these two general aspects to be important for spontaneous structure formation in amphiphilic systems, and future work shall explore the more complex situation, where the chain deformation $X_{1\alpha}X_{1\beta}$ varies in space.

M. M. gratefully acknowledges hospitality at the Kalvi Institute for Theoretical Physics China during the program "Controlled structural formation of soft matter" as well as stimulating discussions with M. Doi, G. H. Fredrickson, W. B. Hu, T. Kawakatsu, T. P. Russell, D. W. Sun, P. Vana, T. Xu, D. Yan, and A. Zippelius. Financial support has been provided by the DFG SFB 937 TP A4. Computations were performed at the Neumann Institute for Computing, Jülich, the HLRN Hannover/Berlin, and the GWDG Göttingen.

*Corresponding author.
mmueller@theorie.physik.uni-goettingen.de

[1] W. H. Li and M. Müller, Annu. Rev. Chem. Biomol. Eng. **6**, 187 (2015).
[2] L. Rockford, Y. Liu, P. Mansky, T. P. Russell, M. Yoon, and S. G. J. Mochrie, Phys. Rev. Lett. **82**, 2602 (1999).
[3] M. P. Stoykovich, M. Müller, S. O. Kim, H. H. Solak, E. W. Edwards, J. J. de Pablo, and P. F. Nealey, Science **308**, 1442 (2005).
[4] M. P. Stoykovich, H. Kang, K. C. Daoulas, G. Liu, C. C. Liu, J. J. de Pablo, M. Müller, and P. F. Nealey, ACS Nano **1**, 168 (2007).
[5] R. A. Segalman, H. Yokoyama, and E. J. Kramer, Adv. Mater. **13**, 1152 (2001).
[6] S. M. Hur, C. J. Garcia-Cervera, E. J. Kramer, and G. H. Fredrickson, Macromolecules **42**, 5861 (2009).
[7] T. Thurn-Albrecht, J. Derouchey, T. P. Russell, and H. M. Jaeger, Macromolecules **33**, 3250 (2000).
[8] Y. Tsori, F. Tournilhac, D. Andelman, and L. Leibler, Phys. Rev. Lett. **90**, 145504 (2003).
[9] Y. Tsori, Rev. Mod. Phys. **81**, 1471 (2009).
[10] M. Gopinadhan, P. W. Majewski, Y. Choo, and C. O. Osuji, Phys. Rev. Lett. **110**, 078301 (2013).
[11] B. McCulloch, G. Portale, W. Bras, J. A. Pople, A. Hexemer, and R. A. Segalman, Macromolecules **46**, 4462 (2013).
[12] D. A. Hajduk, T. Tepe, H. Takenouchi, M. Tirrell, F. S. Bates, K. Almdal, and K. Mortensen, J. Chem. Phys. **108**, 326 (1998).
[13] A. V. M. Zvelindovsky, B. A. C. van Vlimmeren, G. J. A. Sevink, N. M. Maurits, and J. G. E. M. Fraaije, J. Chem. Phys. **109**, 8751 (1998).
[14] D. E. Angelescu, J. H. Waller, D. H. Adamson, P. Deshpande, S. Y. Chou, R. A. Register, and P. M. Chaikin, Adv. Mater. **16**, 1736 (2004).
[15] G. Arya, J. Röttler, A. Z. Panagiotopoulos, D. J. Srolovitz, and P. M. Chaikin, Langmuir **21**, 11518 (2005).
[16] B. L. Peters, A. Ramirez-Hernandez, D. Q. Pike, M. Müller, and J. J. de Pablo, Macromolecules **45**, 8109 (2012).
[17] R. J. Albalak and E. L. Thomas, J. Polym. Sci. B **32**, 341 (1994).
[18] M. A. Villara, D. R. Rueda, F. Ania, and E. L. Thomas, Polymer **43**, 5139 (2002).
[19] T. Xu, J. T. Goldbach, and T. P. Russell, Macromolecules **36**, 7296 (2003).
[20] T. Keller, C. Semmler, and K. D. Jandt, Macromol. Rapid Commun. **29**, 876 (2008).
[21] X. Man, D. Andelman, H. Orland, P. Thébault, P.-H. Liu, P. Guenoun, J. Daillant, and S. Landis, Macromolecules **44**, 2206 (2011).
[22] M. Müller and D.-W. Sun, Phys. Rev. Lett. **111**, 267801 (2013).
[23] K. C. Daoulas and M. Müller, J. Chem. Phys. **125**, 184904 (2006).
[24] D. Q. Pike, F. A. Detcheverry, M. Müller, and J. J. de Pablo, J. Chem. Phys. **131**, 084903 (2009).
[25] M. Müller, J. Stat. Phys. **145**, 967 (2011).
[26] See Supplemental Material at http://link.aps.org/supplemental/10.1103/PhysRevLett.115.228301 for a description of model, numerical techniques, and additional simulation data, which includes Refs. [27–45].
[27] K. C. Daoulas, M. Müller, J. J. de Pablo, P. F. Nealey, and G. D. Smith, Soft Matter **2**, 573 (2006).
[28] F. A. Detcheverry, D. Q. Pike, P. F. Nealey, M. Müller, and J. J. de Pablo, Phys. Rev. Lett. **102**, 197801 (2009).
[29] M. Müller and G. D. Smith, J. Polym. Sci. B **43**, 934 (2005).
[30] B. Steinmüller, M. Müller, K. R. Hambrecht, G. D. Smith, and D. Bedrov, Macromolecules **45**, 1107 (2012).
[31] B. Steinmüller, M. Müller, K. R. Hambrecht, and D. Bedrov, Macromolecules **45**, 9841 (2012).
[32] E. W. Edwards, M. P. Stoykovich, M. Müller, H. H. Solak, J. J. de Pablo, and P. F. Nealey, J. Polym. Sci. B **43**, 3444 (2005).
[33] K. C. Daoulas, M. Müller, M. P. Stoykovich, S. M. Park, Y. J. Papakonstantopoulos, J. J. de Pablo, P. F. Nealey, and H. H. Solak, Phys. Rev. Lett. **96**, 036104 (2006).
[34] E. W. Edwards, M. Müller, M. P. Stoykovich, H. H. Solak, J. J. de Pablo, and P. F. Nealey, Macromolecules **40**, 90 (2007).
[35] K. C. Daoulas, M. Müller, M. P. Stoykovich, H. Kang, J. J. de Pablo, and P. F. Nealey, Langmuir **24**, 1284 (2008).
[36] H. Kang, F. A. Detcheverry, A. N. Mangham, M. P. Stoykovich, K. C. Daoulas, R. J. Hamers, M. Müller, J. J. de Pablo, and P. F. Nealey, Phys. Rev. Lett. **100**, 148303 (2008).
[37] A. M. Welander, H. M. Kang, K. O. Stuen, H. H. Solak, M. Müller, J. J. de Pablo, and P. F. Nealey, Macromolecules **41**, 2759 (2008).
[38] M. P. Stoykovich, K. C. Daoulas, M. Müller, H. M. Kang, J. J. de Pablo, and P. F. Nealey, Macromolecules **43**, 2334 (2010).

[39] S. Ji, U. Nagpal, G. Liu, S. P. Delcambre, M. Müller, J. J. de Pablo, and P. F. Nealey, ACS Nano **6**, 5440 (2012).
[40] U. Nagpal, M. Müller, P. F. Nealey, and J. J. de Pablo, ACS Macro Lett. **1**, 418 (2012).
[41] A. Ramirez-Hernandez, M. Müller, and J. J. de Pablo, Soft Matter **9**, 2030 (2013).
[42] W. H. Li, P. F. Nealey, J. J. de Pablo, and M. Müller, Phys. Rev. Lett. **113**, 168301 (2014).
[43] M. Müller and K. C. Daoulas, Phys. Rev. Lett. **107**, 227801 (2011).
[44] M. Tuckerman, B. Berne, and G. Martyna, J. Chem. Phys. **97**, 1990 (1992).
[45] C. Pangali, M. Rao, and B. Berne, Chem. Phys. Lett. **55**, 413 (1978).
[46] P. J. Rossky, J. D. Doll, and H. L. Friedman, J. Chem. Phys. **69**, 4628 (1978).
[47] M. Müller and K. C. Daoulas, J. Chem. Phys. **129**, 164906 (2008).
[48] L_z is approximately compatible with 5 lamellar periods at $\chi N = 20$. Since $L_y = 10L_z$, the potential maximal mismatch between lamellar period and system size is larger along the z direction than along the y direction. Thus, the system geometry favors the formation of lamellae with normals along the y direction, i.e., opposite to what is observed in simulation.
[49] G. H. Fredrickson, J. Chem. Phys. **117**, 6810 (2002).
[50] T. Shima, H. Kuni, Y. Okabe, M. Doi, X. F. Yuan, and T. Kawakatsu, Macromolecules **36**, 9199 (2003).
[51] The bond anisotropy, $\langle \sum_{i,s} b_{i\beta}(s) b_{i\gamma}(s) \rangle$, of the distribution $\mathcal{P}_o$, which characterizes the noninteracting state, and the lamellar phase at χN and periodicity L_α along the Cartesian direction, α, differ. Therefore, the anisotropy of $\mathcal{P}_o$ cannot be immediately identified with the stress of the lamella structure.
[52] P. E. Rouse, J. Chem. Phys. **21**, 1272 (1953).
[53] M. Doi and S. F. Edwards, *The Theory of Polymer Dynamics* (Oxford University Press, New York, 1994).
[54] P. Ilg, H. C. Öttinger, and M. Kröger, Phys. Rev. E **79**, 011802 (2009).
[55] P. H. Verdier, J. Chem. Phys. **45**, 2118 (1966).
[56] A. Ben-Shaul and I. Szleifer, J. Chem. Phys. **83**, 3597 (1985).
[57] I. Szleifer and M. A. Carignano, Adv. Chem. Phys. **94**, 165 (1996).
[58] M. Müller and M. Schick, Macromolecules **29**, 8900 (1996).
[59] L. Leibler, Macromolecules **13**, 1602 (1980).
[60] P. C. Hohenberg and B. I. Halperin, Rev. Mod. Phys. **49**, 435 (1977).
[61] K. Binder, J. Chem. Phys. **79**, 6387 (1983).